

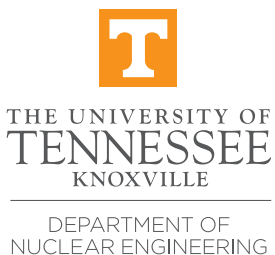
Multiscale Modeling of Fission Gas Bubble Evolution in UO_2 Under Normal Operating Conditions

Brian D. Wirth^{*,#}, D. Andersson¹, S. Blondel, M. Cooper¹, and W. Setyawan²,
on behalf of

Institution	Principal Investigator	Additional Personnel
ANL	Barry Smith	Shashi Aithal
INL	Giovanni Pastore	Cody Permann, Daniel Schwen
LANL	David Andersson**	Danny Perez, Blas Uberuaga
ORNL	David Bernholdt*	Phil Roth
SNL	Habib Najm	
PNNL	Rick Kurtz	Ken Roche, Wahyu Setyawan
UF	Michael Tonks	
UTK	Brian Wirth*	Abdullah Al-Fadhili, Sophie Blondel, Bamin Khomami, Bo Zhang



* bdwirth@utk.edu



Project web site:
<https://collab.cels.anl.gov/display/FissionGasSciDAC2>

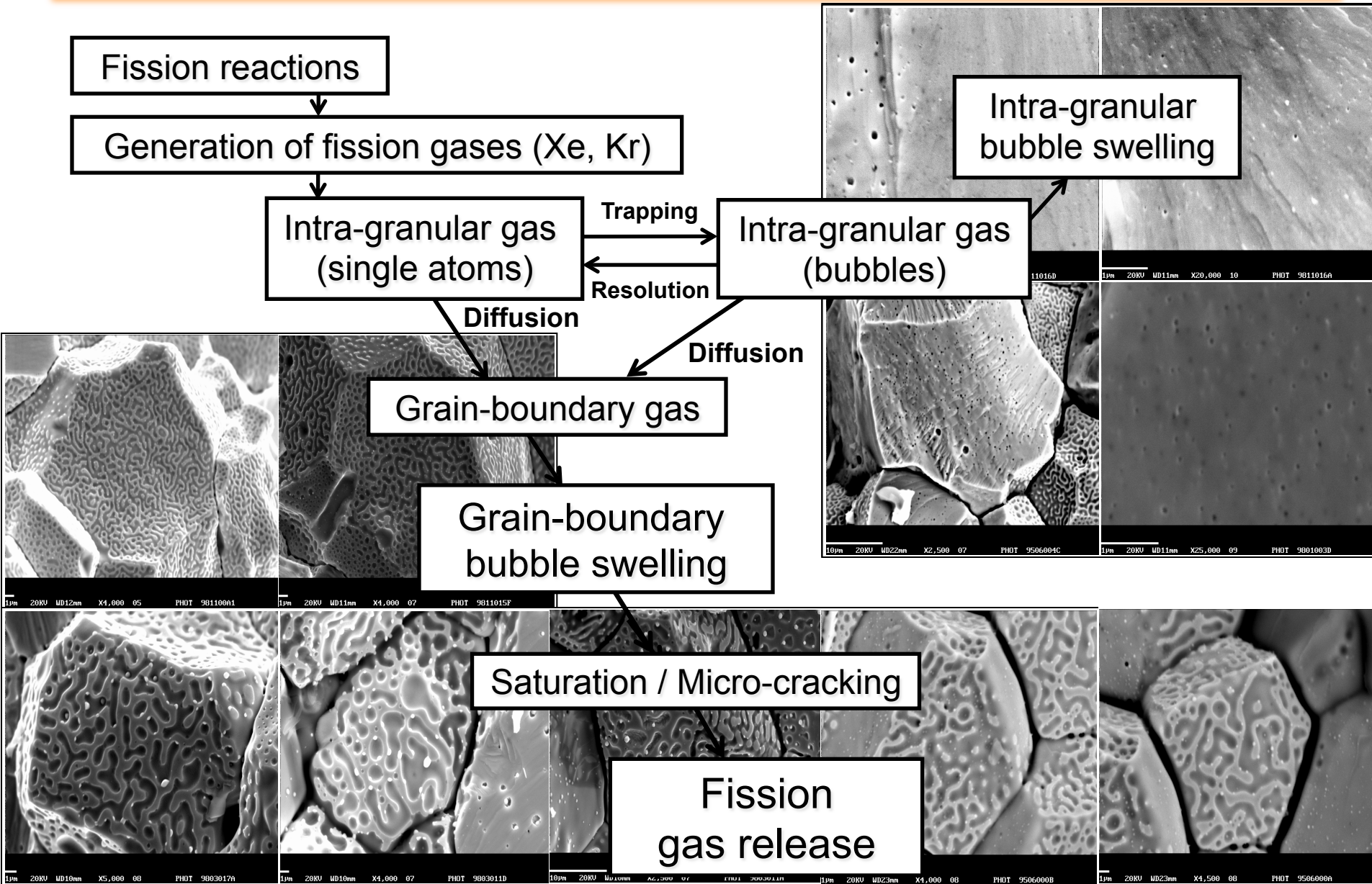


*Presented at the
MRS Spring Meeting
3 April 2018*

This work was supported by the U.S. Department of Energy, Office of Advanced Scientific Computing Research, and the Office of Nuclear Energy as part of the Scientific Discovery through Advanced Computing (SciDAC).



Introduction: the long-standing fission gas problem

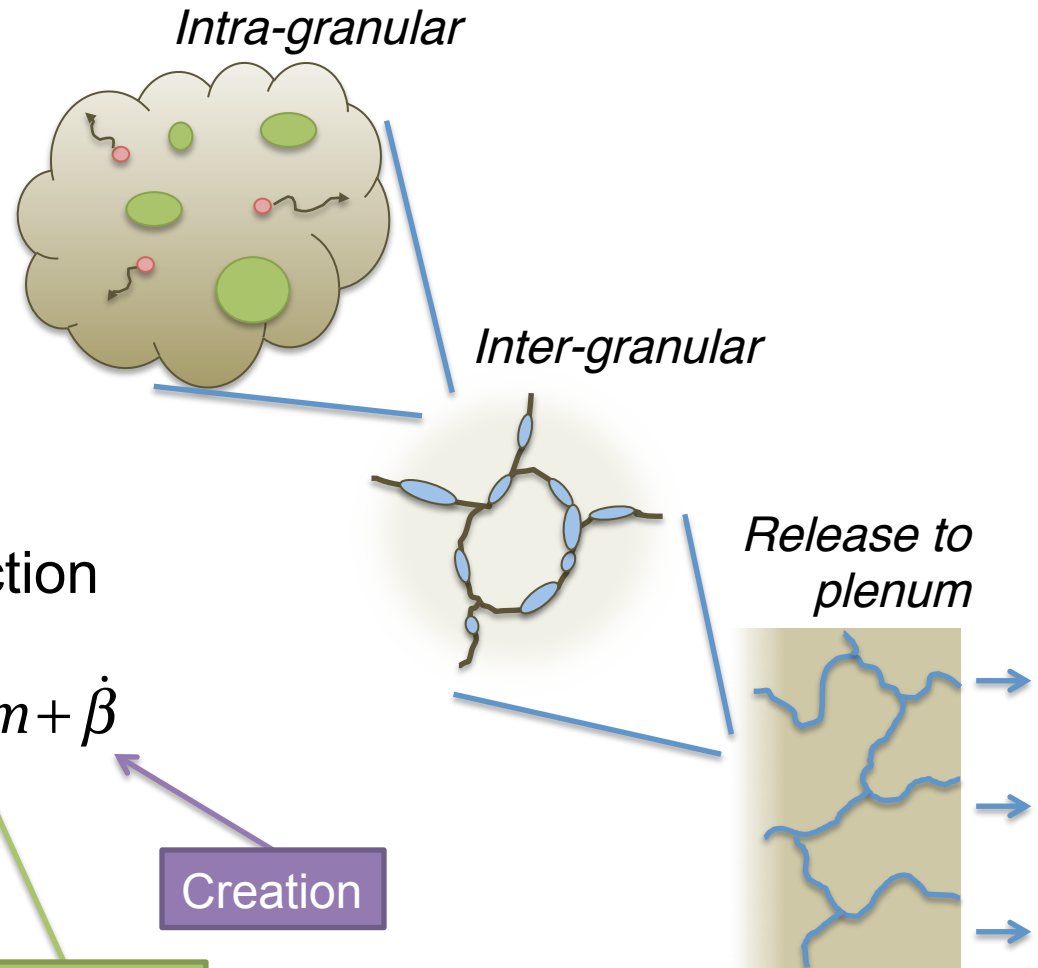


* G. Pastore (INL) – micographs from White, Corcoran and Barnes, Report R&T/NG/EXT/REP/02060/02 (2006).

Introduction: the long-standing fission gas problem

- Fission gas located:

- Mobile single gas atoms
- *Intra-granular* bubbles
- *Inter-granular* bubbles



- Gas release driven by inter-granular bubble interconnection

$$\frac{\partial c}{\partial t} = D\nabla^2 c - gc + b'm + \dot{\beta}$$

Diagram illustrating the components of the gas release equation:

- Diffusion** (blue box) points to $D\nabla^2 c$
- Absorption** (red box) points to $-gc$
- Re-solution** (green box) points to $b'm$
- Creation** (purple box) points to $\dot{\beta}$

- Effective diffusion rate: $D' = Db' / (b' + g)$

Fission gas bubble observations

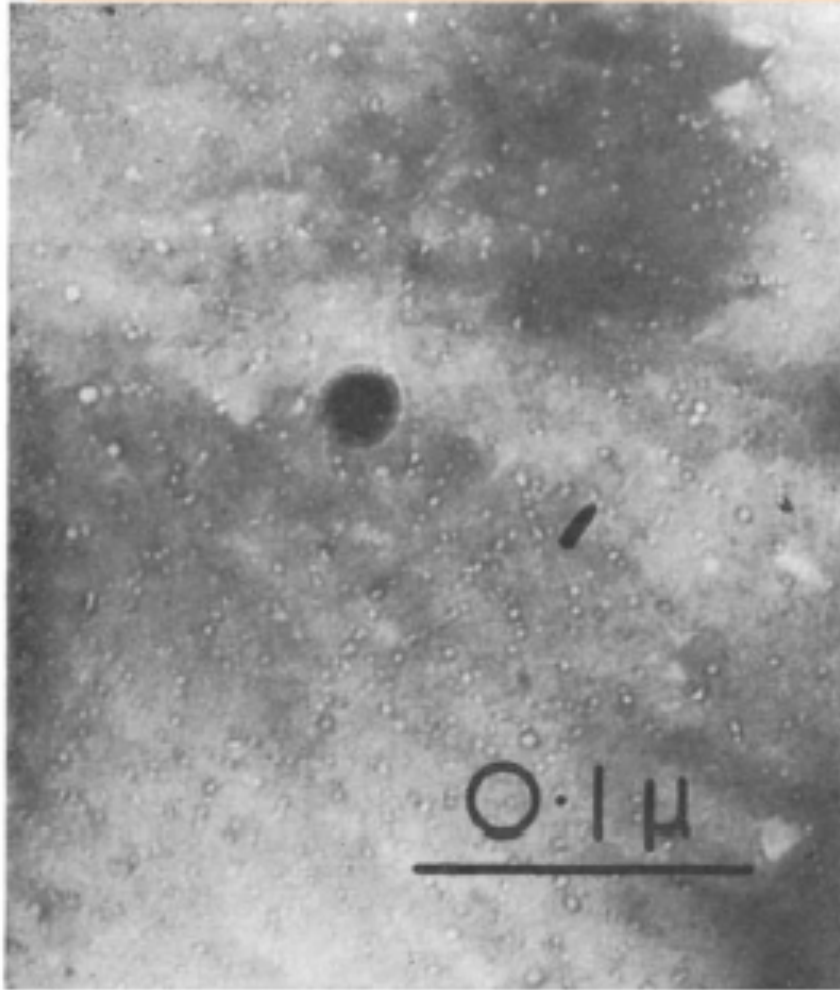


Fig. 2. Transmission electron micrograph of typical intragranular gas bubbles in uranium dioxide irradiated at a rating of $\approx 6.8 \times 10^{18}$ fissions/m²·sec to a burn up of $\approx 3.2 \times 10^{25}$ fissions/m³. The estimated irradiation temperature was ≈ 1600 °C. $\times 300\,000$

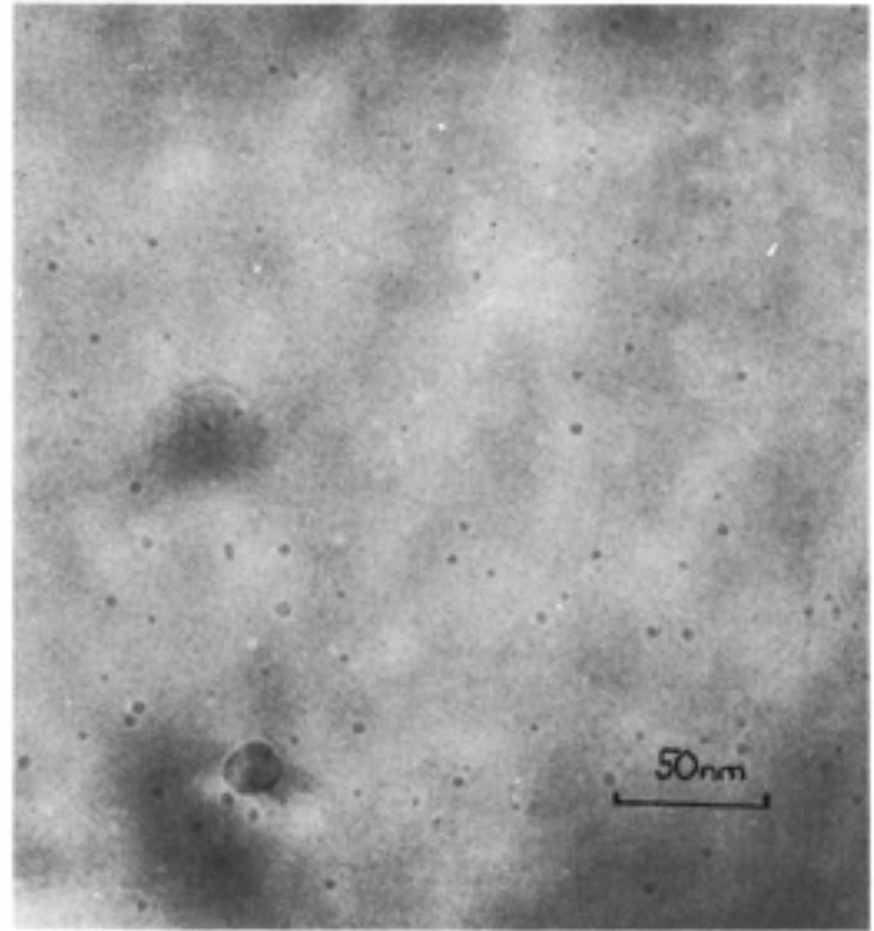
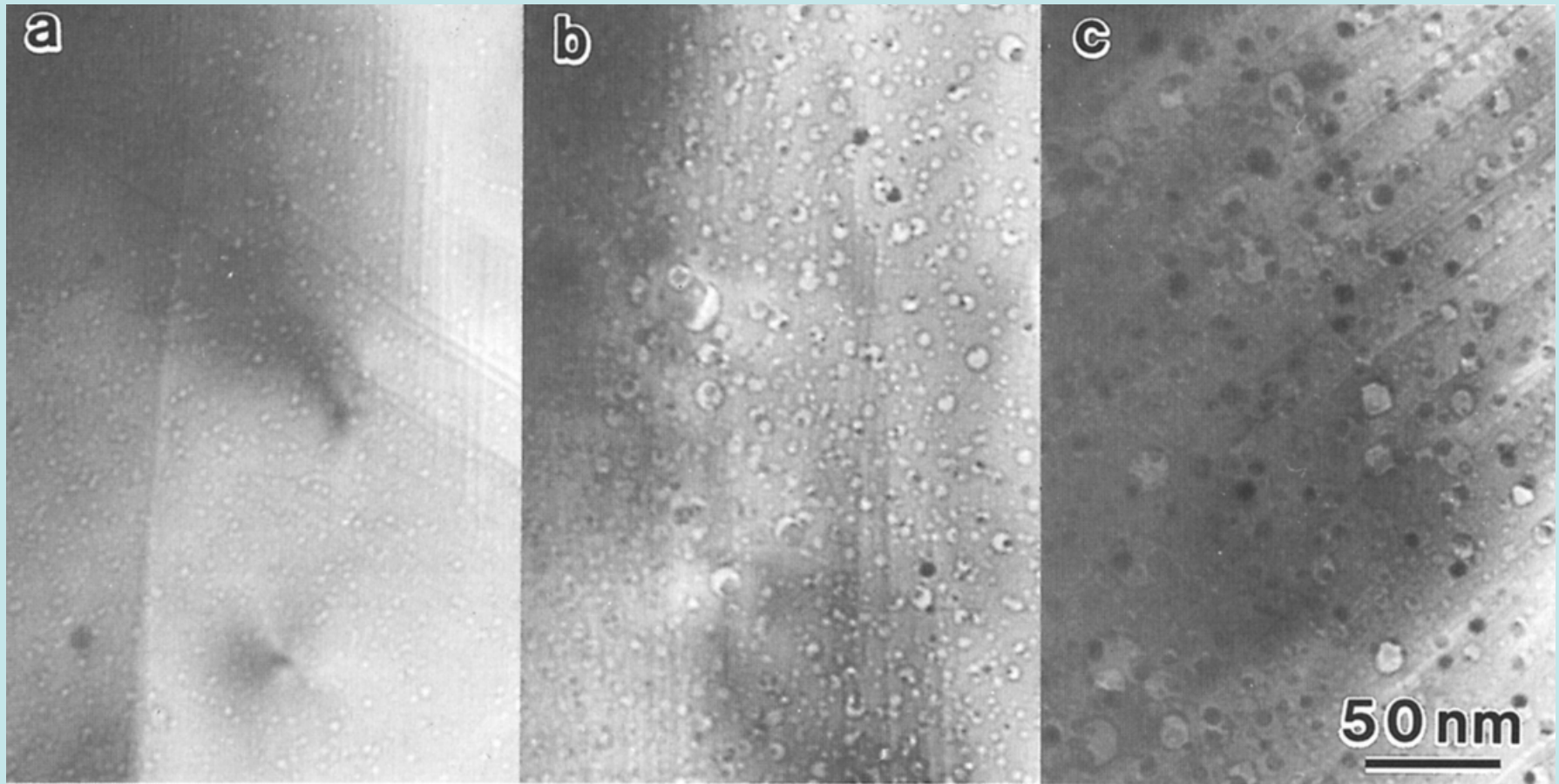


Fig. 7. Transmission electron micrograph taken over-focus of a thin foil from pin 3 at an irradiation temperature of 1560°C . The gas bubbles are at a lower density than in pins 1 and 2 and the tendency to nucleate in lines is not apparent.

Fission gas bubble observations



23 GWd/t

44 GWd/t

83 GWd/t

Fission gas challenges

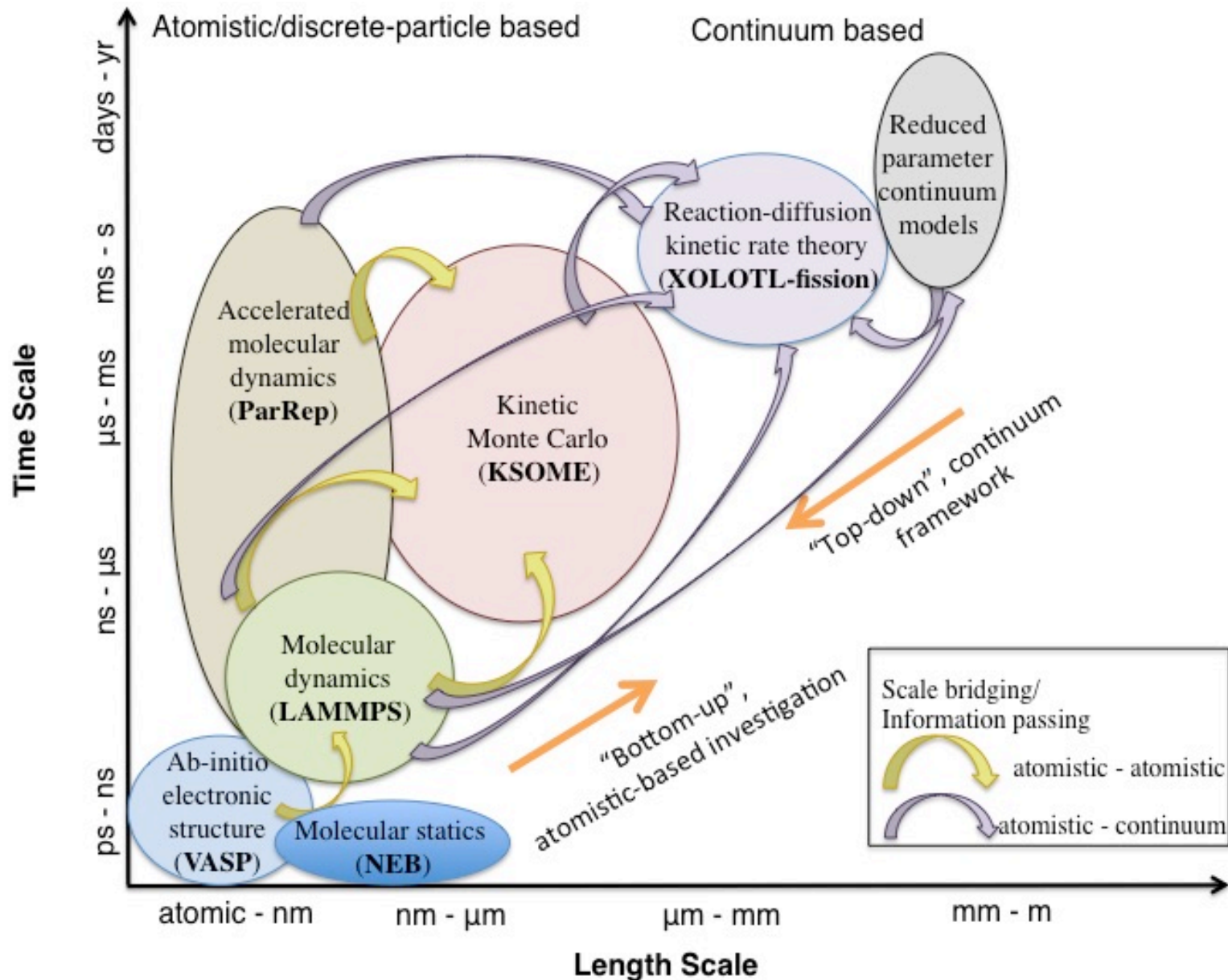
- Current, engineering scale models do not do a good job of predicting fission gas release and gas bubble contributions to swelling but are of paramount importance – well recognized problem in fuel performance modeling:

- Lösönen* states in recent review: “In transients in particular, when pronounced bubble coarsening takes place, the release rate depends strongly on the development of the characteristics of the bubble population”, and “a mechanistic approach in modeling the bubble coarsening process should be applied.”
- Pastore** performed an uncertainty quantification assessment in BISON and concluded “a better characterization of the parameters through through experimental and theoretical research may reduce the uncertainty in fission gas behavior calculations and in the multiple related aspects of fuel performance analysis” and further noted that there is at least a factor of 2X uncertainty in current engineering predictions of fission gas release

*Lösönen, *JNM* **280** (2000) 56-72.

Pastore, Swiler, Hales, Novascone, Perez, et al., *JNM* **456 (2015) 398-408.

Our vision of multiscale modeling



Xe diffusion mechanisms

Current empirical model:

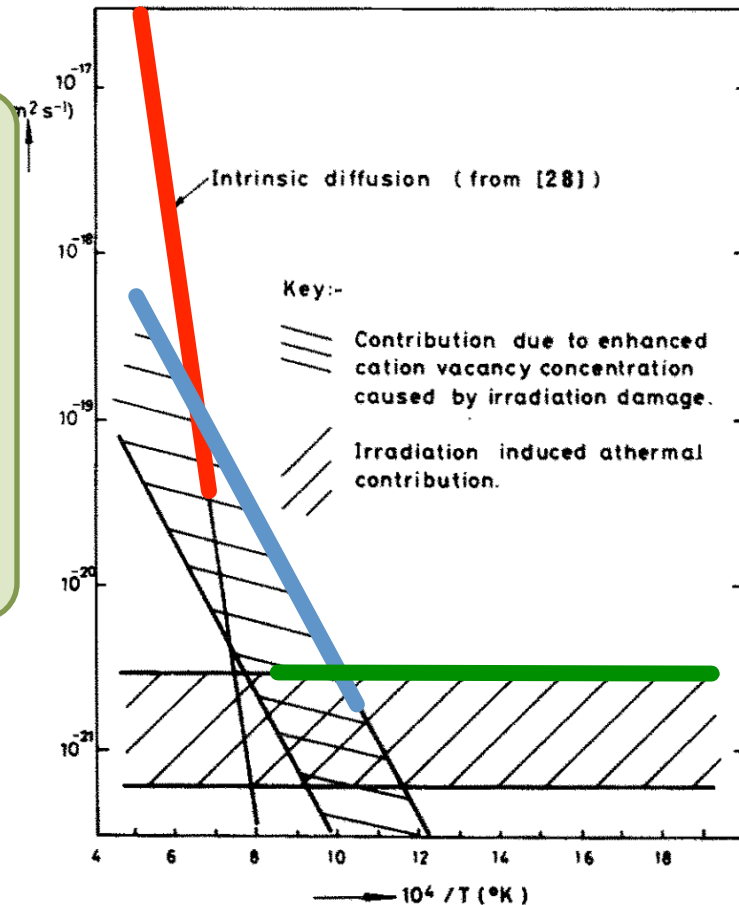
Total: $D_{\text{Xe}} = D_1 + D_2 + D_3$

Intrinsic: $D_1 = 7.6 \cdot 10^{-10} \times \exp(-3.04 / k_B T) \text{ [m}^2/\text{s]}$

Irr. Enhanced: $D_2 = 4 \times 1.4 \cdot 10^{-25} \times \sqrt{\dot{F}} \exp(-1.2 / k_B T) \text{ [m}^2/\text{s]}$

Athermal: $D_3 = 4 \times 2 \cdot 10^{-40} \times \dot{F} \text{ [m}^2/\text{s]}$

- Empirical relationships.
- The mechanisms for D_1 , D_2 , and D_3 are not fully understood, which complicates development of predictive models.
- D_1 and D_2 driven by vacancy population, similar to U behavior.
- D_3 is believed to be caused directly by damage.



J. A. Turnbull et al., JNM 107, 168 (1982)

Goal: Calculate D_1 and D_2 fission gas diffusion through simulation using **point defect dynamics** and D_3 by direct MD simulations.

Governing reaction-diffusion equations

- D_1 and D_2 calculated by combining empirical potentials and DFT calculations to parameterize reaction-diffusion equations formulated to be consistent with phase-field models, e.g.:

Diffusion (Xe_{U2O}):
$$\left(\frac{\partial y_{\text{XeU}_2\text{O}}}{\partial t} \right)_D = \nabla \cdot (M_{\text{XeU}_2\text{O}} y_{\text{XeU}_2\text{O}} \nabla (\mu_{\text{XeU}_2\text{O}} - (2\mu_U + \mu_O)))$$

Cluster formation (Xe_{U2O}):
$$\left(\frac{\partial y_{\text{XeU}_2\text{O}}}{\partial t} \right)_{R_1} = y_{\text{XeUO}} y_{\text{VU}} \frac{M_{\text{VU}}}{S^2} \cdot Z (\mu_{\text{XeU}_2\text{O}} - (\mu_{\text{XeUO}} + \mu_{\text{VU}}))$$

Reactions with interstitials (Xe_{U2O}):
$$\left(\frac{\partial y_{\text{XeU}_2\text{O}}}{\partial t} \right)_{R_2} = -y_{\text{XeU}_2\text{O}} y_{\text{UI}} \left(\frac{M_{\text{XeU}_2\text{O}}}{S^2} + \frac{M_{\text{UI}}}{S^2} \right) \cdot Z (\mu_{\text{XeU}_2\text{O}} + \mu_{\text{UI}} - (\mu_{\text{XeUO}} + \mu_{\text{VI}} + \mu_{\text{UI}}))$$

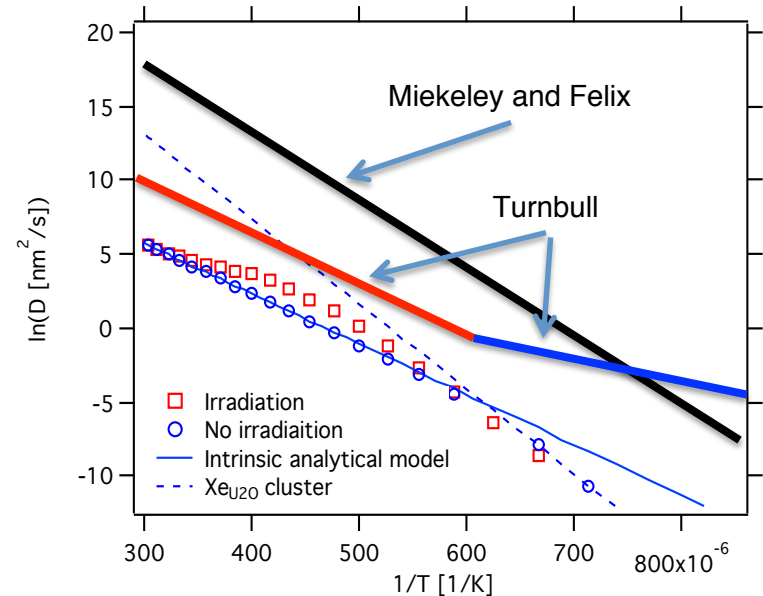
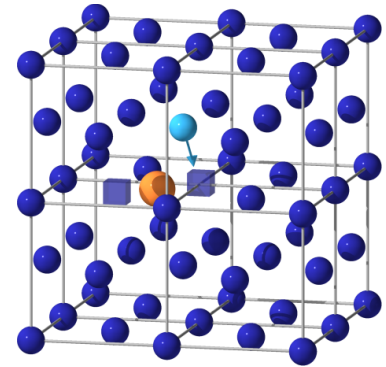
Production and reaction with sinks/sources (V_U):
$$\left(\frac{\partial y_{\text{VU}}}{\partial t} \right)_{R_1} = K_{\text{VU}} - M_{\text{VU}} y_{\text{VU}} k_{\text{VU}}^2 (\mu_{\text{VU}} - \mu_{\text{UU}}) - \left(\frac{M_{\text{VU}}}{S^2} + \frac{M_{\text{UI}}}{S^2} \right) Z y_{\text{VU}} y_{\text{UI}} \cdot (\mu_{\text{VU}} + \mu_{\text{UI}} - (\mu_{\text{UU}} + \mu_{\text{VI}}))$$

Chemical potential differences, free energies and mobilities from DFT/MD:

$$\mu_A - \mu_B = \frac{\delta}{\delta y_A} \left(\int_{\Omega} G_m^{\text{Total}} d\Omega \right)_{y_B} = \left(\frac{\partial G_m^{\text{Total}}}{\partial y_A} \right)_{y_B} - \nabla \cdot \left(\frac{\partial G_m^{\text{Total}}}{\partial \nabla y_A} \right)_{y_B}$$

Point defect evolution in irradiated UO_2

- Initial point defect dynamics model
 - Uranium vacancies (mono- and di-)
 - Uranium interstitials
 - Equilibrium oxygen (stoichiometric)
 - Xenon residing in uranium single vacancy(+oxygen) and diffusing as a di-vacancy
 - Damage source term (uranium interstitials, vacancies)
 - Sinks (static bubble population)
- Xe/Vacancy cluster dominates low temperature diffusion



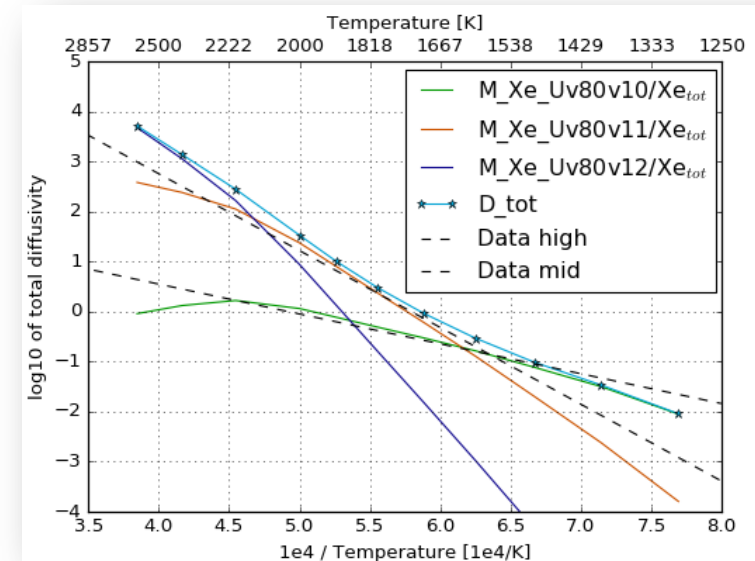
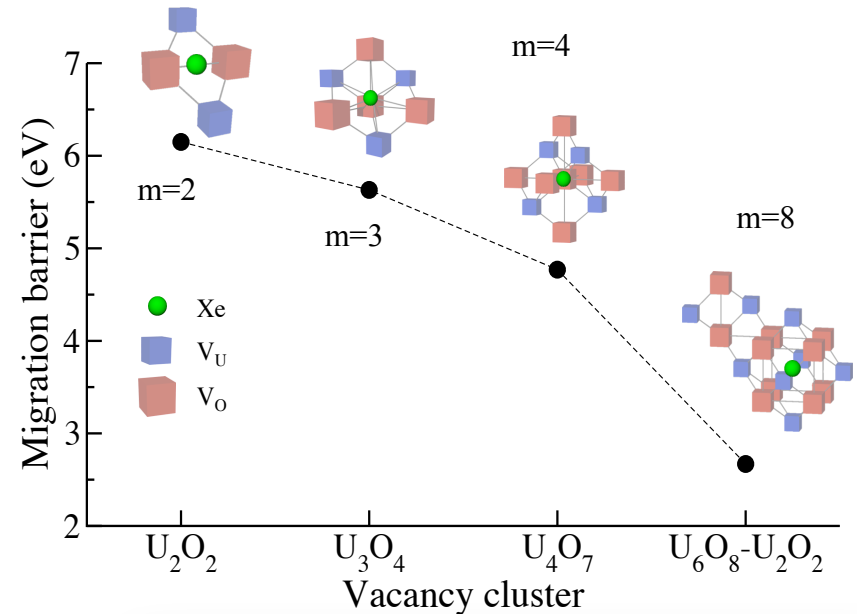
Xe+2V diffusion behavior does not capture experiments

M. R. Tonks, et al., Comput. Mater. Sci. 51 20 (2012)
D. A. Andersson, et al., JNM 451, 225 (2014)
D. A. Andersson et al., Phys. Rev. 84, 054105 (2011)
D. A. Andersson et al., JNM 462, 15 (2015)

Migration properties as function of cluster size

- **Preliminary results indicate that the mobility increases for increasing cluster size.**
- **The stable Xe_{U6O8} cluster moves by binding two additional vacancies.**

Preliminary estimates from statics calculations of the migration barrier for different vacancy clusters in UO_2 .

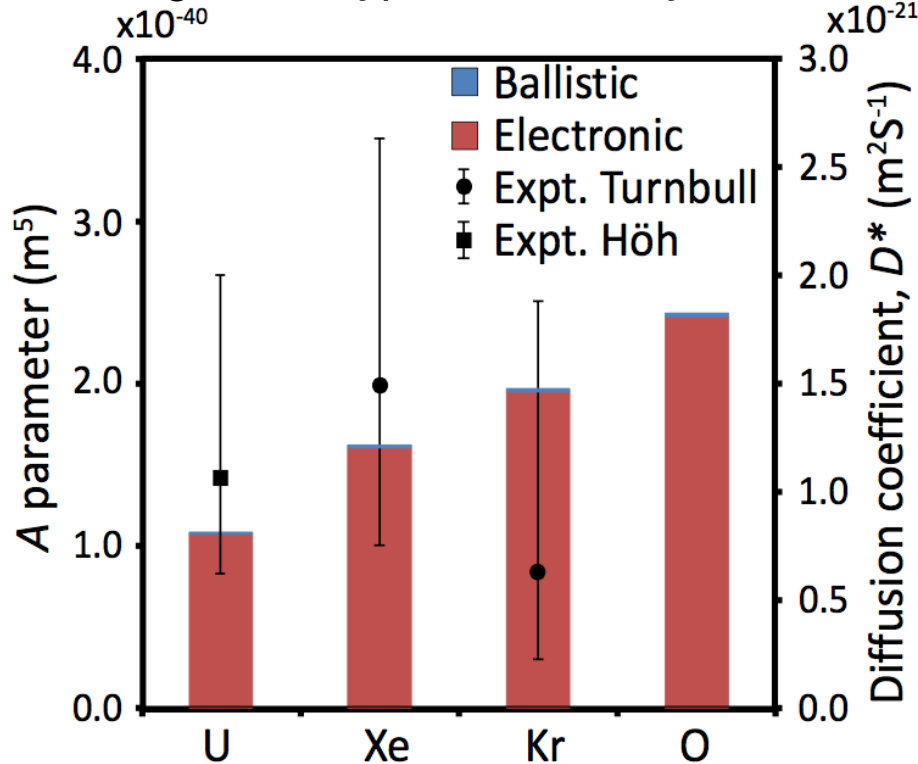


Xe+Uv8Ov10 Vacancy drives intermediate diffusion (D_2)

D_3 : Fission gas migration under irradiation

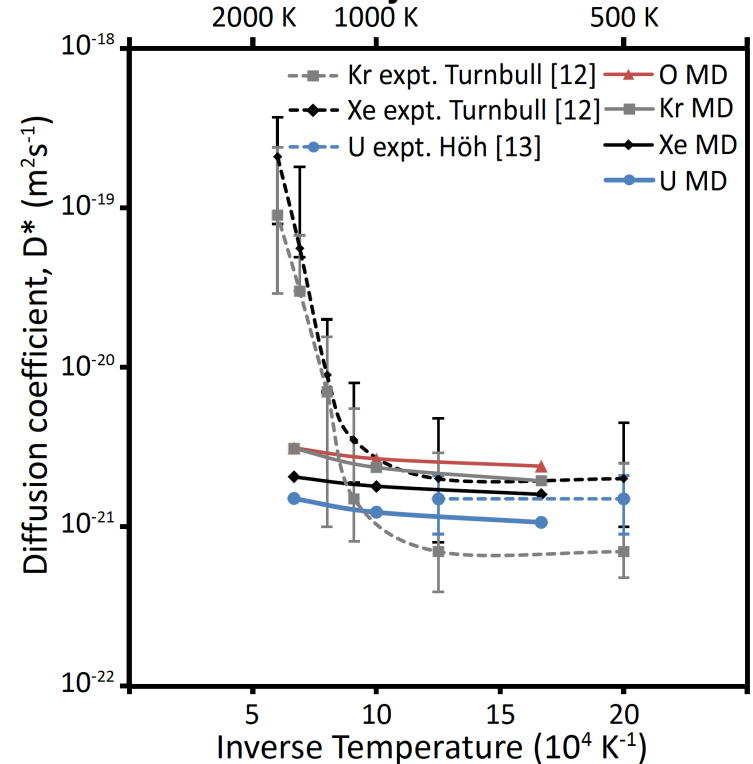
Left axis diffusivity per fission rate

Right axis typical diffusivity in reactor



$$D^* = (A_B + A_E)\dot{F}$$

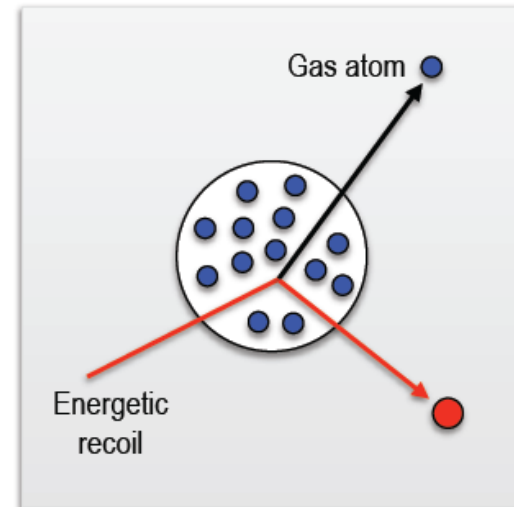
Temperature dependence of the diffusivity



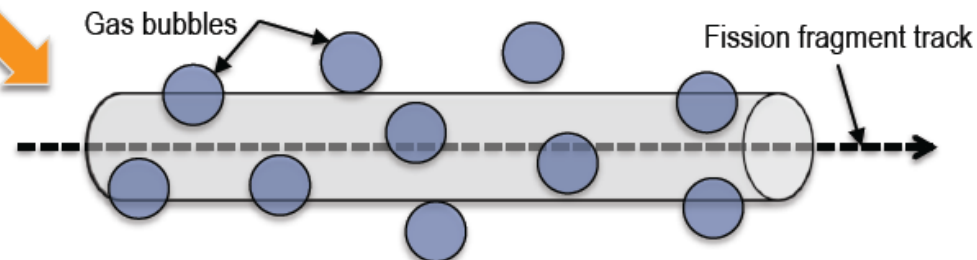
Diffusion for cation, O, Xe and Kr in UO₂, ThO₂ and PuO₂. Near-athermal mechanism and within scatter of experiment. Ratio of 10:1 for ratio of electronic to ballistic contribution. Little difference between actinide oxides.

Fission gas bubble re-resolution mechanisms

- In homogeneous re-resolution, individual gas atoms are ejected from the gas bubble through collisions with energetic fission fragments or recoil uranium atoms that are traversing the bubble
- The kinetic energy acquired by gas atoms through these collisions can range up to the maximum ballistic energy of a fission fragment
- For re-resolution to be achieved a gas atom must acquire energy above a critical value E_{\min}
- In the heterogeneous model bubbles are almost completely destroyed by the passage of a fission fragment in the vicinity of a bubble
- The destruction of the bubble occurs through either the vaporization of the dense gas due to the passing pressure wave or to the trapping of gas atoms in material thrown from one side of the bubble to the other
- This mechanism requires modeling of the entire interaction of the bubble with the fission thermal spike

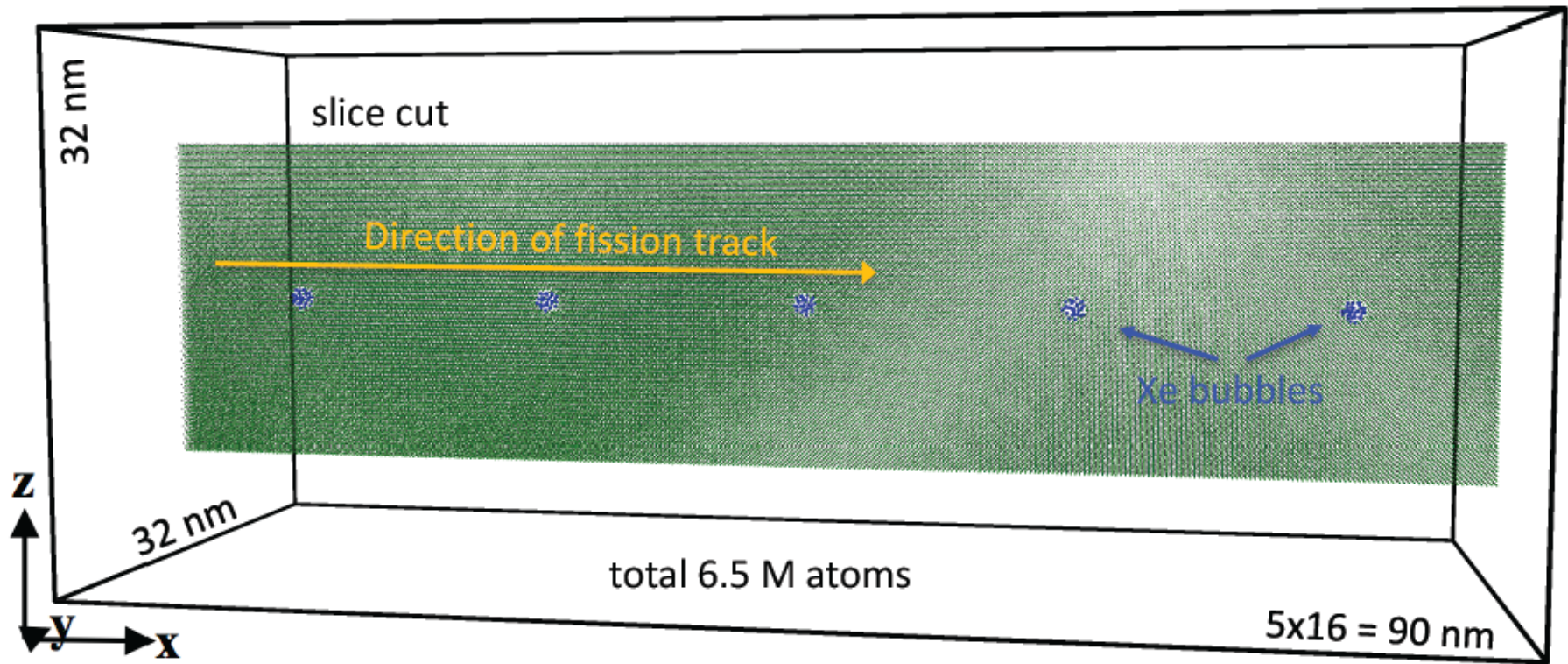


$$b_{\text{hom}} = \mu_{\text{ff}} \dot{F} \frac{2\pi Z^4 e^2}{E_{\text{ff}}^{\text{max}} E_{\min}} \ln \left(\frac{E_{\text{ff}}^{\text{max}}}{E_{\min}} \right) = \sim 4 \times 10^{-6} / \text{s}$$



$$b_{\text{het}} = \pi (R_b + R_{\text{ff}})^2 (2\dot{F}\mu_{\text{ff}}) = \sim 1.5 \times 10^{-3} / \text{s}$$

MD simulations of heterogeneous resolution



- Interatomic potentials:
 - UO₂: 2014 Cooper potential^[1].
 - Xe-UO₂: 2016 Cooper potential^[2].
 - Xe: 2003 Tang-Toennies potential^[3].
- Thermal spike radius = 4 nm^[4].
- Simulation at 600 K.
- Bubbles are filled with gaseous Xe atoms.

[1] W. D. Cooper, et al., *J. Phys.: Condens. Matt.* **26**, 105401 (2014).

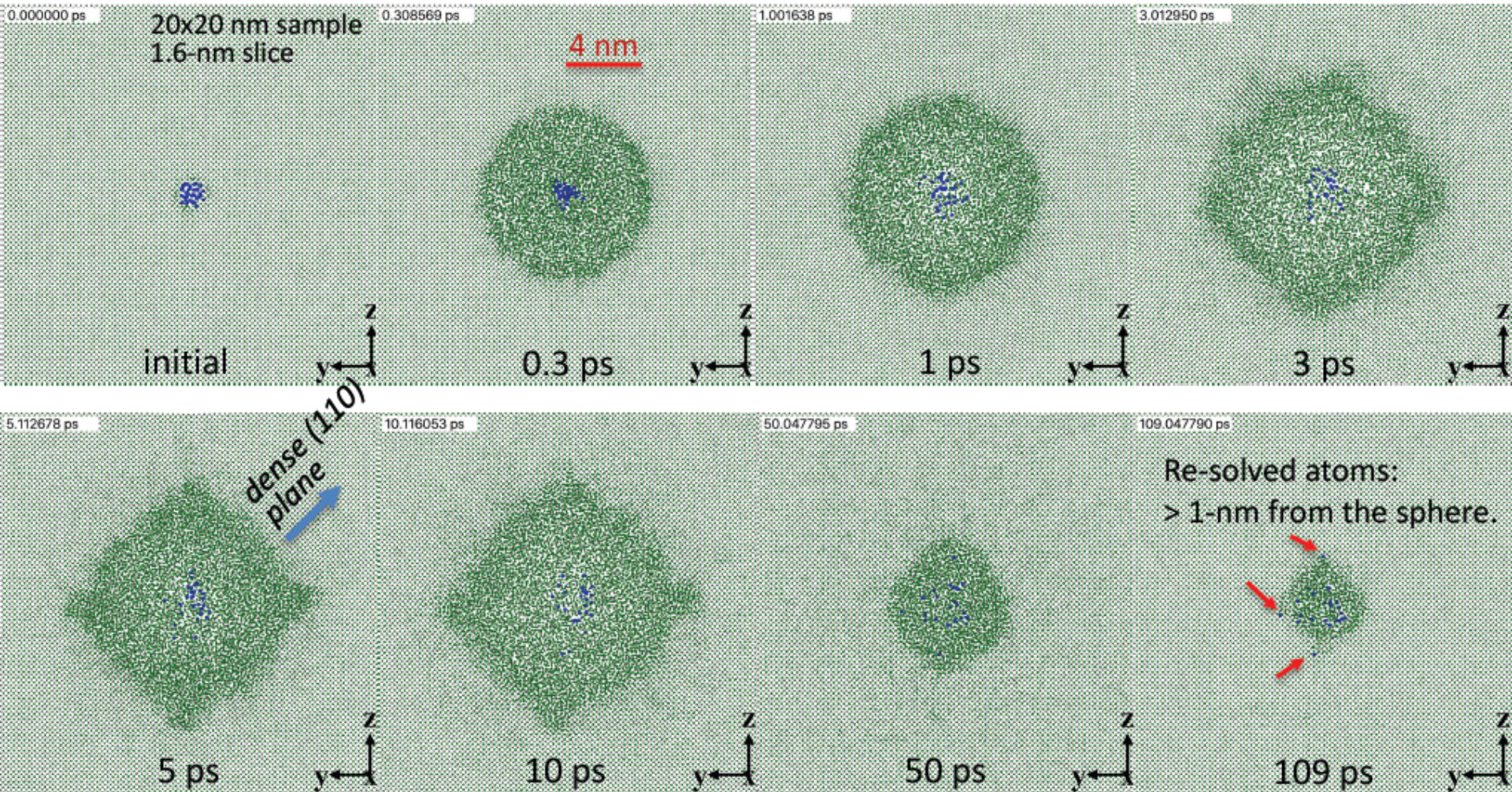
[2] W. D. Cooper, et al., *J. Phys.: Condens. Matt.* **28**, 405401 (2016).

[3] K. T. Tang and J. P. Toennies, *J. Chem. Phys.* **118**, 4976 (2003).

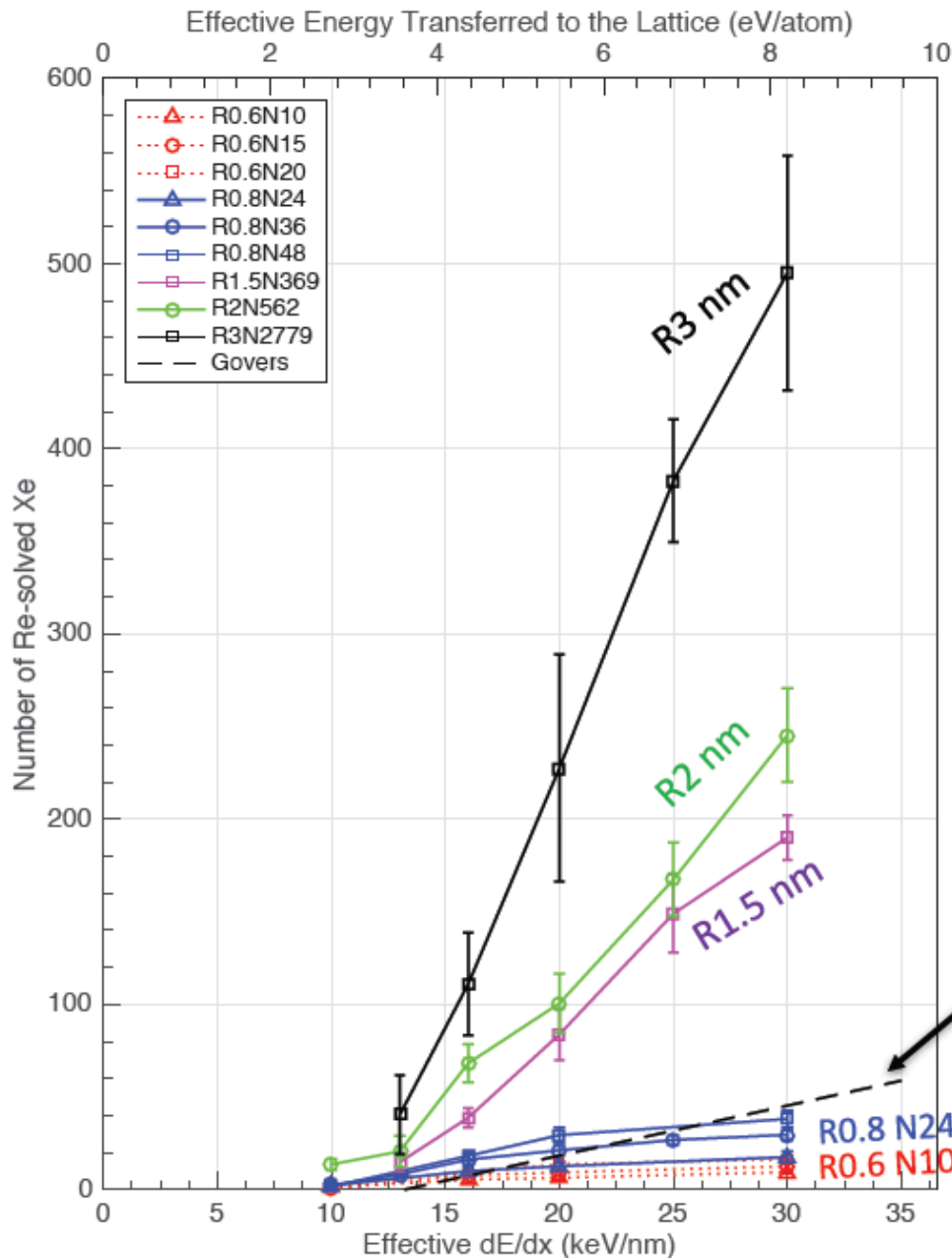
[4] based on e-ph coupling constant $\lambda = 4$ nm from Toulemonde et al, NIMB 166 (2000) 903.

MD simulations of heterogeneous resolution

R0.8N36 bubble subjected to 16 keV/nm thermal spike.



MD simulations of size dependent resolution

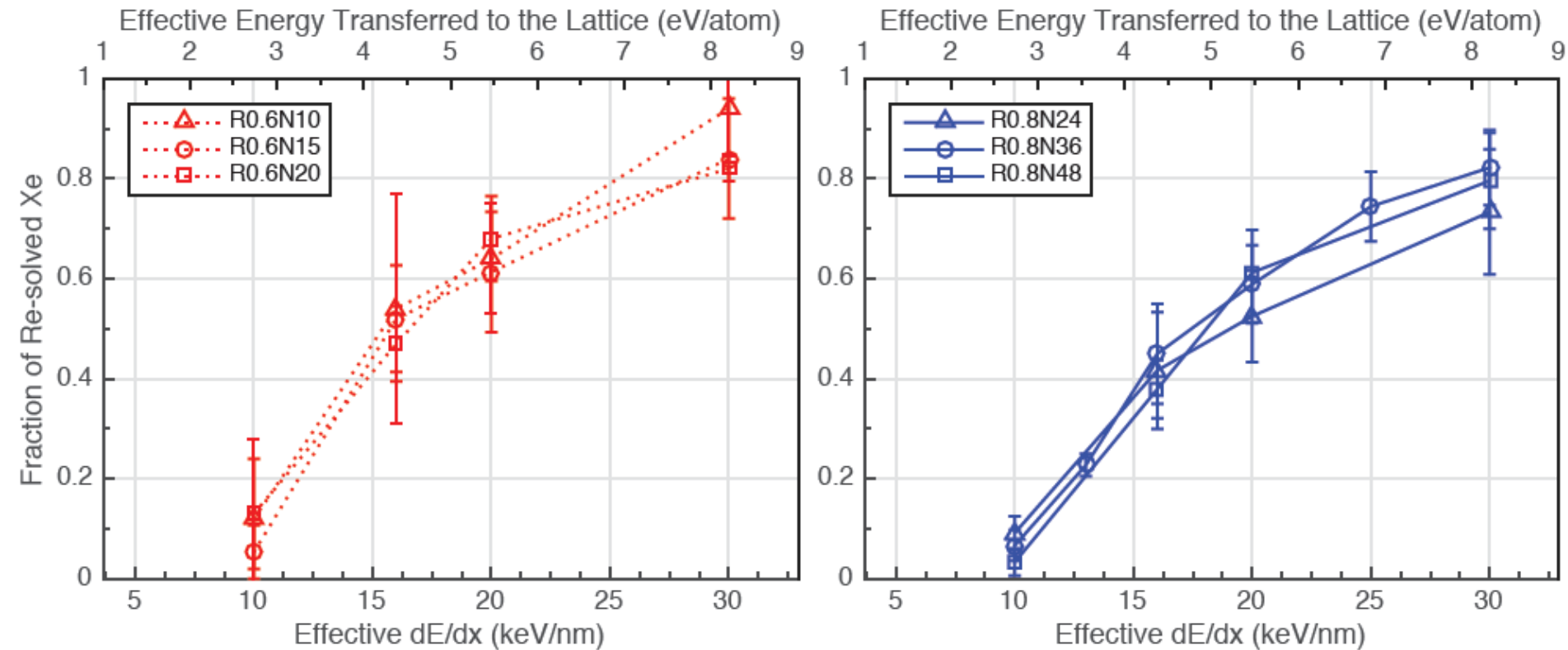


Bubble size \uparrow $N_{\text{re-sol}} \uparrow$

Govers' model (independent of R):
[JNM 420, 282 (2012)]
 $N_{\text{re-sol}} = 2.7 (dE/dx_{\text{eff}} - 13.2)$

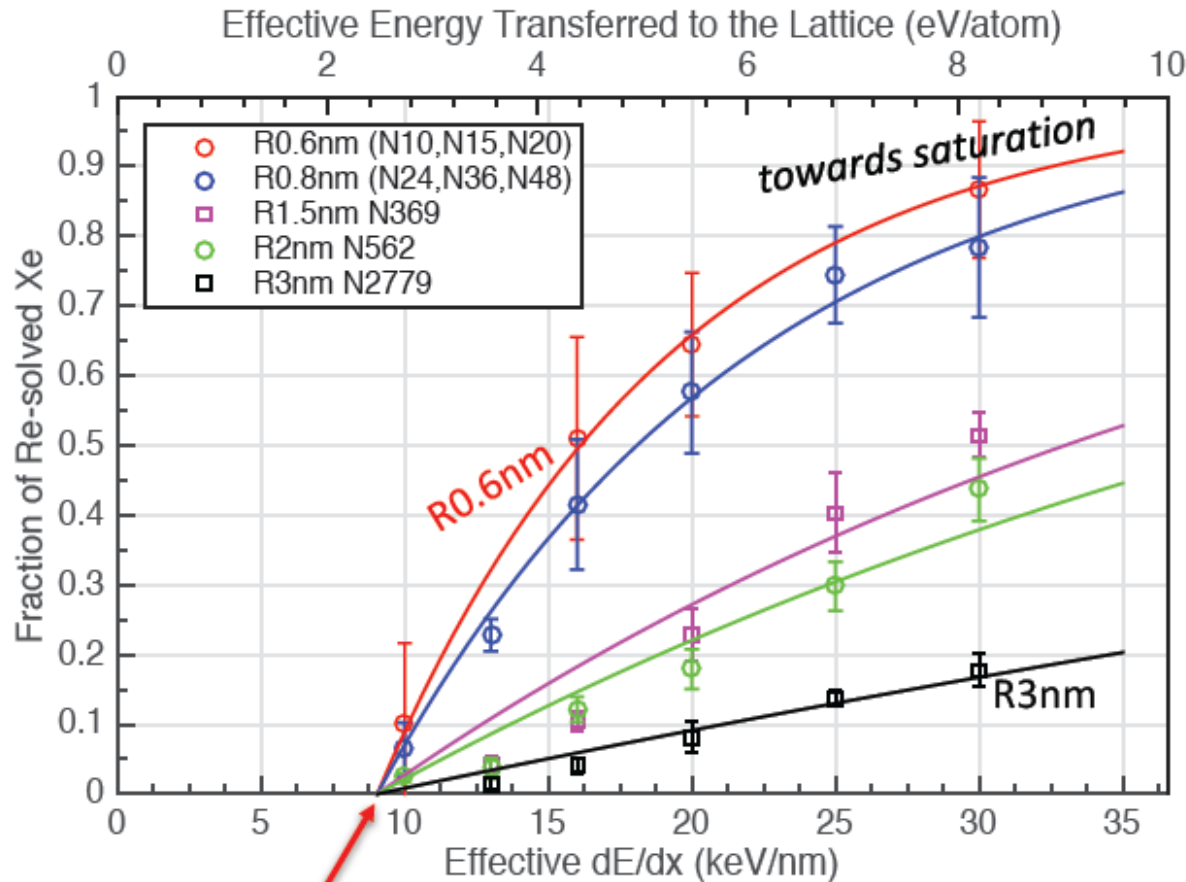
MD simulations of pressure dependent resolution

Gas densities $\sim 11, 17, 22 \text{ Xe/nm}^3$



Fraction of re-solved Xe does not depend on Xe density, consistent with Govers's observation.

MD simulations of dE/dx (S_e)



Fit model:
 $y = 1 - \exp(-\alpha(x - x_c))$

Fit results:
 $x_c = 9.042$ keV/nm

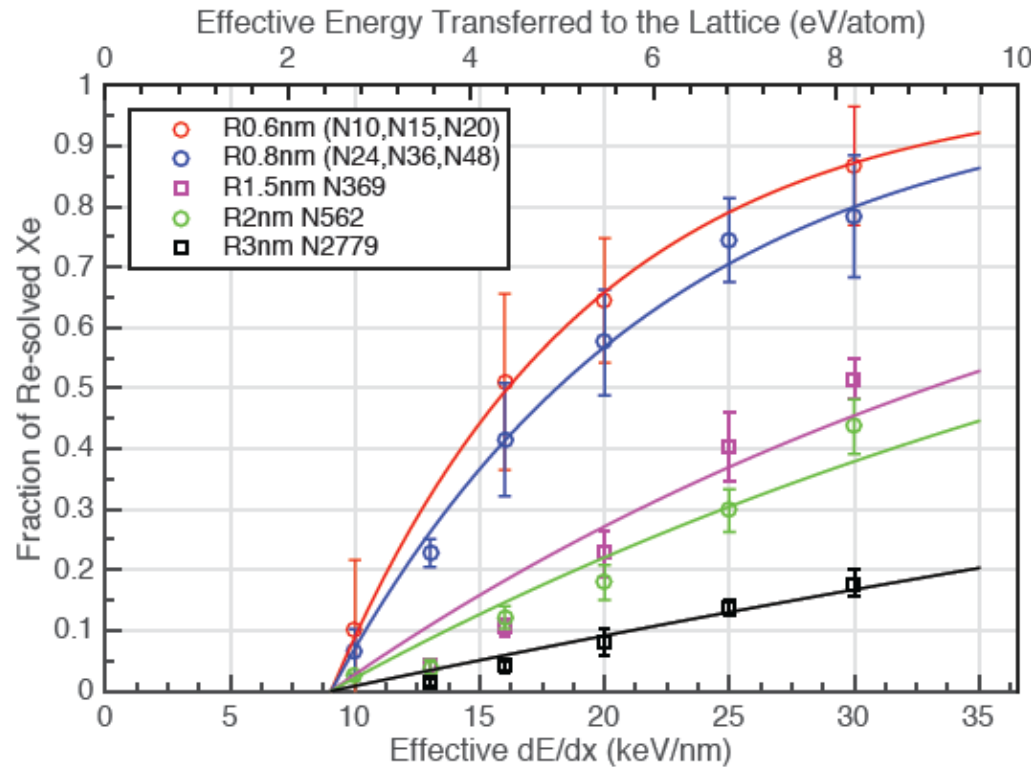
R (nm)	α (nm/keV)	R ² of the fit
0.6	0.09798	0.98
0.8	0.07662	0.98
1.5	0.02893	0.89
2	0.02273	0.94
3	0.00874	0.95

Saturation
coefficient.

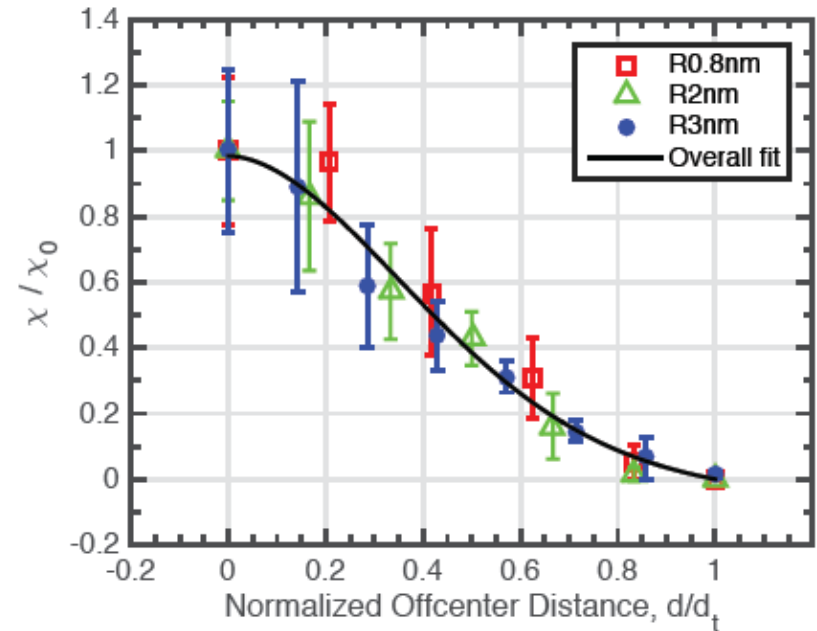
No re-solution below $x_c = 9.042$ keV/nm

Fission gas bubble re-resolution

On-center Data



Off-center Efficiency



$$\eta \equiv \frac{\int_0^1 y(2\pi x) dx}{\int_0^1 (2\pi x) dx} \approx 0.25$$

$$N_{\text{res}} = 0.25N\{1 - \exp[-0.1967 \cdot (S_{\text{eff}} - 9.042) \cdot \exp(-1.1756R)]\}$$

N_{res} is the number of re-solved Xe.

N is the number of Xe in the bubble.

R is the bubble radius in nm.

S_{eff} is the effective electronic dE/dx transferred to the lattice in keV/nm.

Updated fission gas re-resolution model

$$N_{\text{res}}/N = 0.25 \{1 - \exp[-0.1967(S_{\text{eff}} - 9.042) \exp(-1.1756R)]\} \approx 0.09 \quad \leftarrow \begin{array}{l} R = 1 \text{ nm} \\ S_{\text{eff}} = 16 \text{ keV/nm} \end{array}$$

Turnbull's model of re-resolution rate:

$$b_{\text{het}} \equiv \underbrace{\pi(R_b + R_f)^2}_{\text{area of influence}} \underbrace{(2\dot{F}\mu_f)}_{\substack{\text{fission rate} \\ \text{density}}} \underbrace{(\text{completely re-solved})}_{\text{range of fission gas}} \approx 1.5 \times 10^{-3} / \text{s} \quad \leftarrow \begin{array}{l} R_b = R_f = 1 \text{ nm} \\ \dot{F} = 10^{-8} \text{ nm}^{-3}\text{s}^{-1} \\ \mu_f = 6 \mu\text{m} \end{array}$$

Should be modified to:

$$b_{\text{het}} \equiv \pi(R_b + R_f)^2 (2\dot{F}\mu_f) * 0.25 \{1 - \exp[-0.1967(S_{\text{eff}} - 9.042)e^{-1.1756R_b}]\}$$

$$b_{\text{het}} \equiv \pi(R_b + R_f)^2 (2\dot{F}\mu_f) * \frac{1}{\mu_f} \int_0^{\mu_f} 0.25 \{1 - \exp[-0.1967(S_{\text{eff}} - 9.042)e^{-1.1756R_b}]\} dx$$

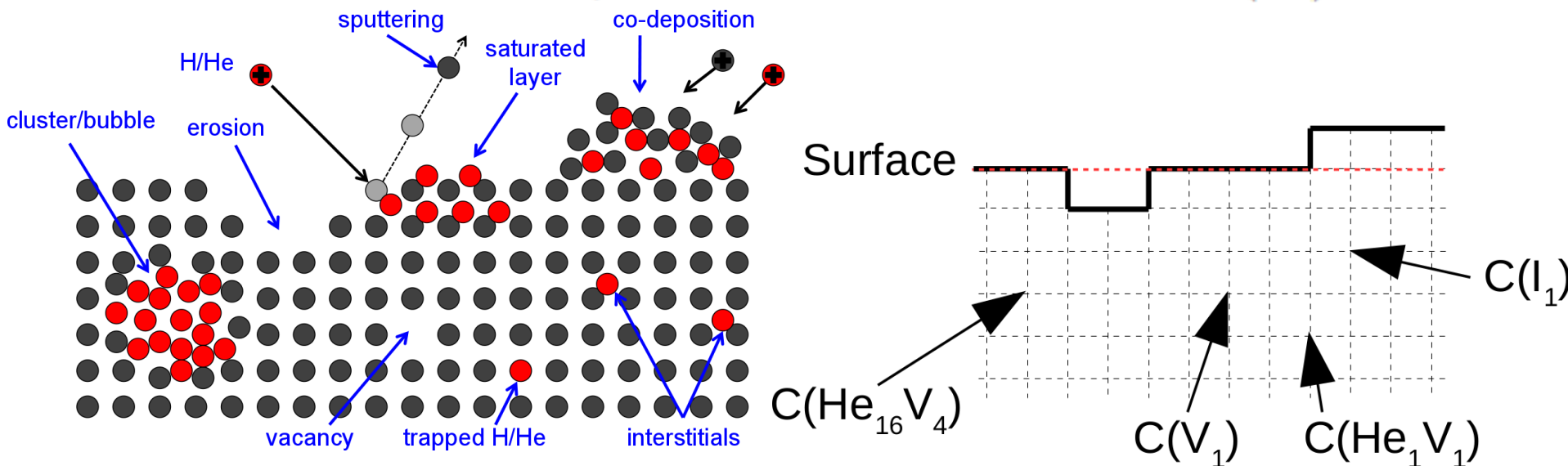
for $S_{\text{eff}} > 9.042 \text{ keV/nm}$, else the integrant = 0. depend on x

Xolotl*

- Xolotl (SHO-lottle) is the Aztec god of lightning and death
- Developed from 'scratch' for the SciDAC project, designed for HPC (current and emerging architectures – multicore, multicore+accelerator) to solve advection – reaction – diffusion cluster dynamics problems within spatially-resolved continuum domain (C++ with MPI and independent modules for physics, solvers and data management)
- 2D and 3D recently implemented
- Model considers continuum concentration of He, vacancies, interstitials and mixed clusters at spatial grid points, solving the coupled advection-reaction-diffusion equations



$$\delta_t \bar{C} = \phi \cdot \rho + D \nabla^2 \bar{C} - \nabla \bar{v} C - \bar{Q}(\bar{C})$$

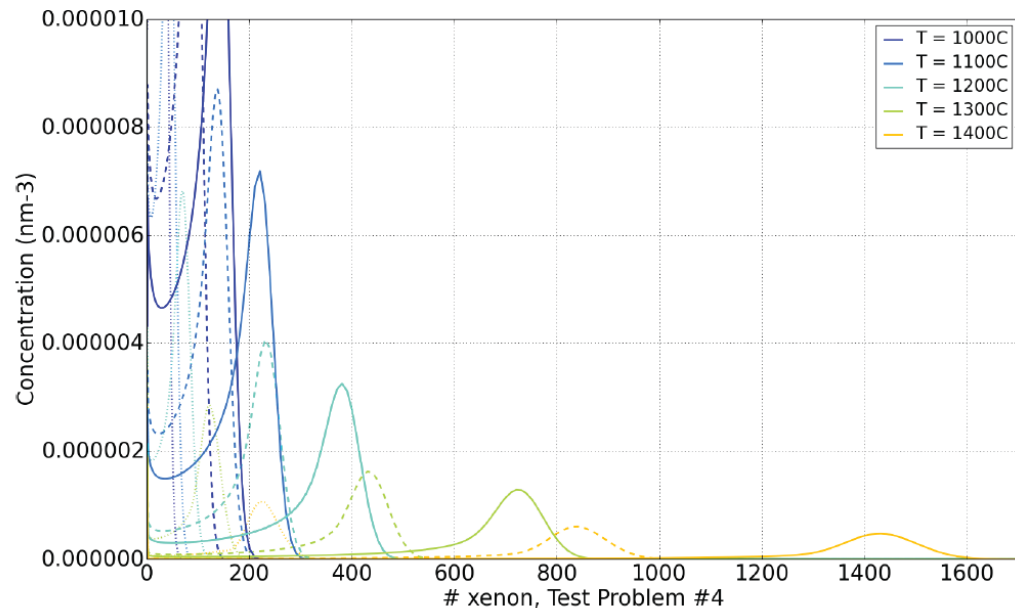
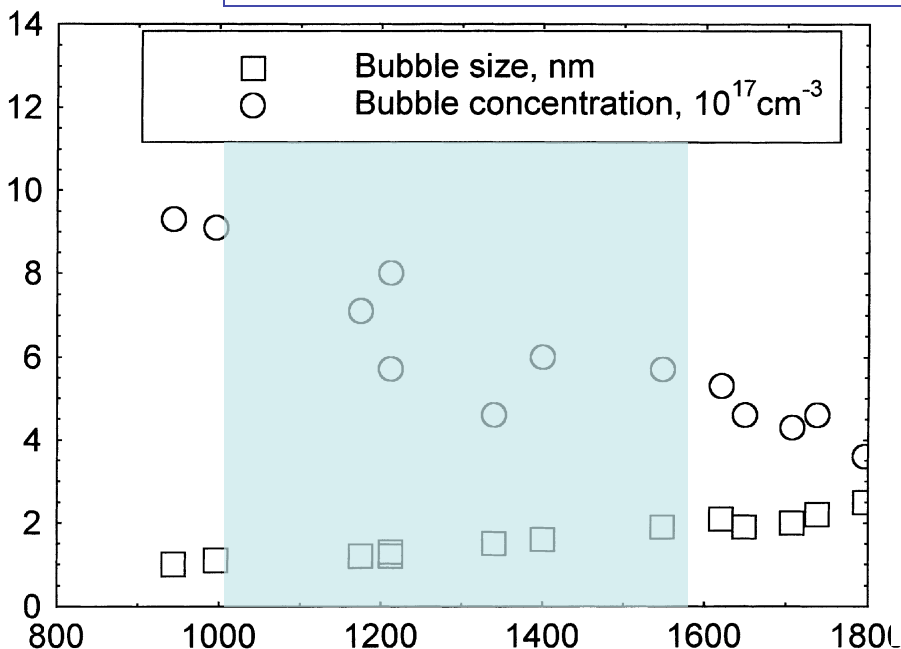


Fission gas evolution modeling

- Developed a suite of test problems at low to higher burnup to begin testing/evaluating the continuum approaches & connecting detailed bubble populations to reduced order models

Test problem:

- No spatial dependence,
 - Xe introduced at $2\text{E}18 \text{ m}^{-3}\text{s}^{-1}$ (Fission rate $\sim 8\text{E}18 \text{ m}^{-3}\text{s}^{-1}$)
 - Model ~ 2 years ($7\text{E}7$ seconds), corresponding to $\sim 0.83\%$ burnup - 7.9 GWd/ton
- Temperatures of 1000, 1100, 1200, 1300, 1400 and 1560°C
- Monitor bubble size, mean size as function of Temperature

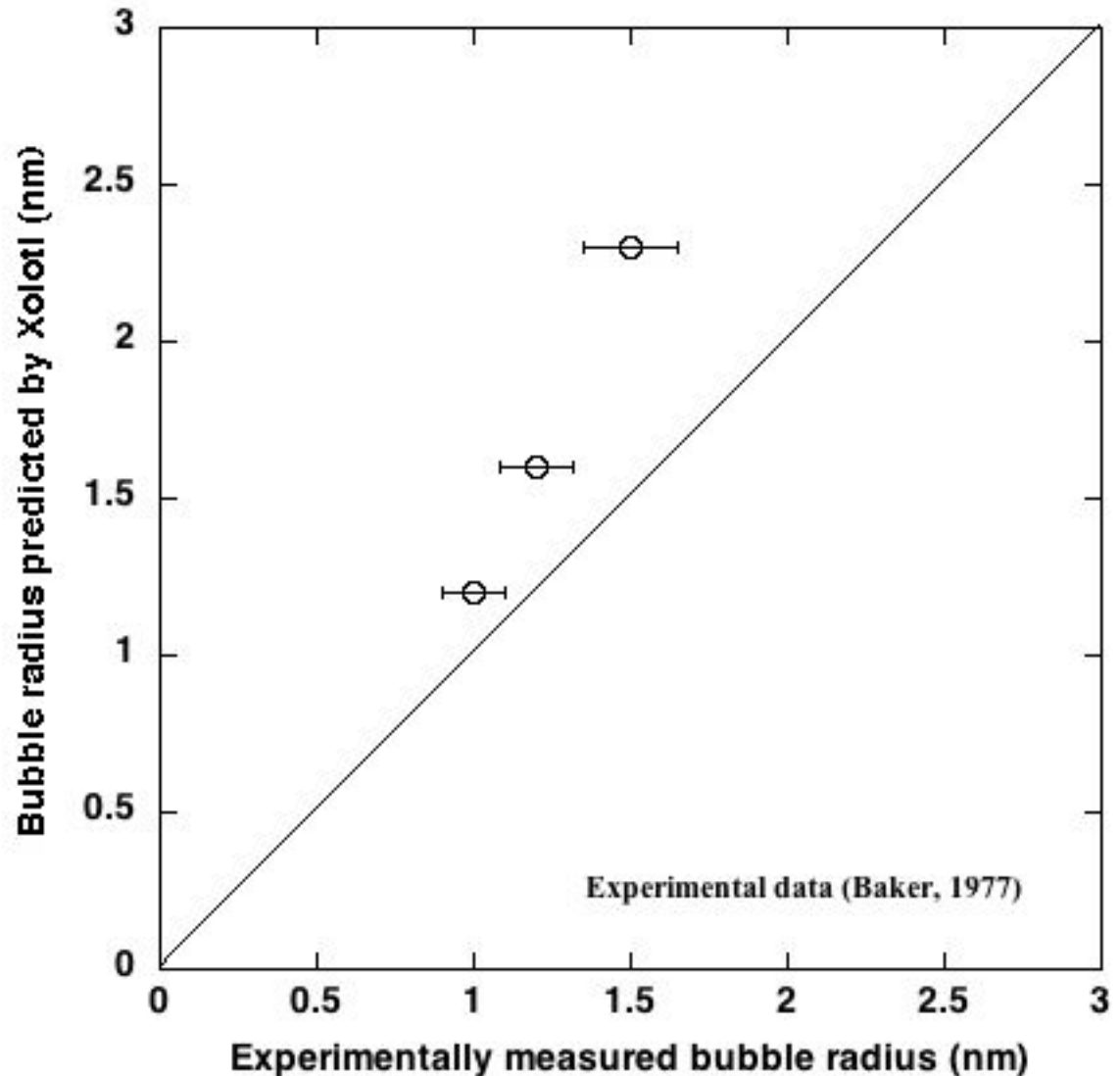


Temperature, °C

*Baker, *JNM* **66** (1977) 283-291.

Initial Xolotl predictions

- Initial Cluster Dynamics modeling results (without re-solution) are representative in terms of intragranular bubble density and size
- Provide a platform for uncertainty quantification/ sensitivity analysis on Xe diffusion mechanisms/ diffusivity
- Future efforts will expand spatially-dependent modeling to predict both intra-granular and inter-granular bubble formation & inform reduced parameter models (c.f., Pastore presentation)



Summary

- **Multiscale approach involving both an atomistic, ‘bottom-up’ perspective along with simultaneous ‘top-down’ modeling to improve understanding of long-standing problem of fission gas diffusion and bubble evolution mechanisms leading to fission gas release**

Initial conclusions:

- **Fission gas diffusion mechanisms under irradiation remains uncertain, but evidence points to vacancy-cluster mediated diffusion at higher temperatures and radiation-enhanced diffusion at lower irradiation temperatures**
- **Re-resolution of gas atoms dominated by heterogeneous resolution, but bubble dissolution is not complete – newly derived model has a threshold dE/dx & is sensitive to bubble size & track overlap with bubbles**
- **Developing spatially-dependent cluster dynamics for Xe fission gas bubble populations – initial results promising, but need to demonstrate influence of re-resolution and spatial dependence to provide “computational database” for reduced parameter models**
- **Need to extend beyond intra-granular bubbles – plans to couple to phase field (MARMOT) for grain boundary bubble evolution**

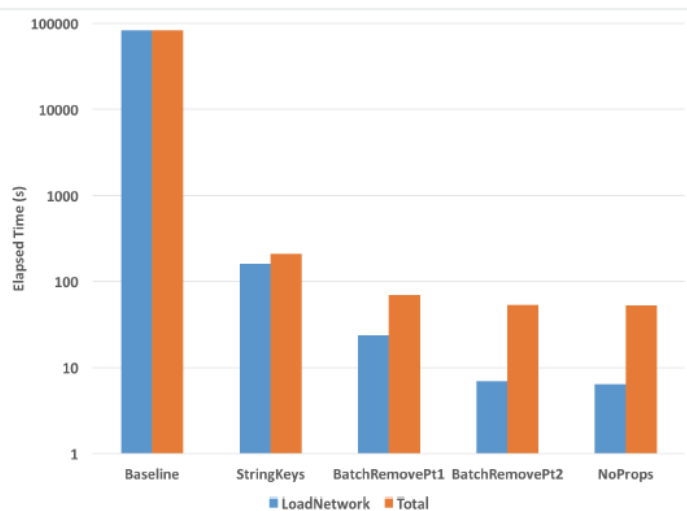
Improving computational efficiency of Xolotl for modeling gas bubble evolution in nuclear materials

Philip C. Roth, ORNL, rothpc@ornl.gov
David Bernholdt, ORNL, bernholdtde@ornl.gov
Sophie Blondel, UT-Knoxville, sbldondel@utk.edu
Brian Wirth, UT-Knoxville, bdwirth@utk.edu
& NE-SciDAC Pilot team

Problem

- Xolotl reaction-diffusion cluster dynamics code developed within Plasma Surface Interactions (PSI) SciDAC project and adapted for nuclear fuel simulation in NE-SciDAC-Pilot project with collaboration from SciDAC Institute for Sustained Performance, Energy, and Resilience (SUPER)
- Xolotl reaction network initialization did not scale well with respect to problem size
 - Adequate performance for smaller PSI reaction networks
 - Desired NE test problem scales were intractable due to poor reaction network initialization performance

Reaction network initialization time (blue) and total run time (orange) for NE test problem, performed on Oak Ridge Leadership Computing Facility's Eos system. Left-to-right, bars indicate performance of initial, baseline version to optimized version. Note elapsed times are plotted on a log scale.



Approach

- Diagnosed performance bottlenecks using Xolotl's built-in performance infrastructure
- Modified reaction network lookup maps to use key strings instead of composition maps – cheaper to compare and enables reuse
- Made supercluster reactant grouping more efficient by removing many reactants at once and eliminating redundant examination of known reactants

Impact

- Optimizations reduced Xolotl reaction network initialization time for nuclear fuel applications from 23+ hours to under 7 seconds (improvement of 10^4 times)

Performance improvements benefit both NE-SciDAC-Pilot and the OFES-PSI versions of Xolotl, enabling initial comparisons of bubble radii predicted by Xolotl with experimental results

